

The Evaluation of Reliability of Strength Data for Functionally Gradient Material Considering Effective Volume

Yasuyoshi FUKUI

(Received May 31, 1994)

ABSTRACT

Reliability of functionally gradient material (FGM) concerning with the brittle fracture strength is studied based on the "weakest link" model. The FGM is the plaster-corundum model system having four kinds of composition gradation. Effects of the specimen size and shape, i.e., the stress gradation, on the strength are numerically analyzed and discussed based on the experimental results of 3-point bending, 4-point bending, and ring diametrical compression tests. The applied stress is divided into two parts, i.e., acted on a matrix of plaster and distributed particles of corundum, based on the micro-mechanics. The fracture strength of plaster, which dominates the strength of specimen itself, is plotted on the Weibull probability paper and each data set is confirmed to obey the two-parameter Weibull distribution. The average of Weibull parameter of $m=8$ is obtained then the deviation of data is relatively large. The dependence of the effective volume on the composition gradation is analyzed and seems to have a tendency to increase as the composition gradation increased. The strength of plaster is independent on the composition gradation. The mean strength of plaster, $\bar{\sigma}$, is decreased with the increase of the effective volume, V_E , and is arranged as the relation of $\bar{\sigma} = 8.3 V_E^{-0.125}$.

1. INTRODUCTION

The reliability of functionally gradient material (FGM), which have non-uniform tailored composition gradation to satisfy the required function from a machine and/or a structural design, is one of the important factor for a promotion of the commercial usage. One of the aim to make composition gradation is development of the mechanical properties by combining the advantage of strong but brittle material with relatively weak but ductile material. It seems to happen to possess only the brittle character even those designed materials. Then it is necessary to consider the evaluation method of the brittle character properly to apply brittle FGMs as a structural member. The data of fracture strength and the discussion of reliability concerning with FGMs seem to be impossible to find out yet because of the newness of itself. Thus, it is interesting to analyze the reliability of brittle FGMs connecting with the size effect of strength.

The author proposed one of the method to make a FGM ring or thick-walled tube by applying a centrifugal force to the mixture of molten metal and ceramics powder⁽¹⁾⁻⁽²⁾. The justice of this method was confirmed with a FGM of plaster-corundum model system. And then, the effects of composition gradation on the ring crushing strength were measured and

analyzed using the plaster-corundum FGMs⁽³⁾. The simplest theory to evaluate the strength of brittle material statistically seems to be the weakest link model, i.e., Weibull theory⁽⁴⁾⁻⁽⁶⁾. The brittle character of the size effect can be explained by applying the concept of effective volume. The plaster itself must obey the weakest link theory and the strength of the model FGM depends on the fracture strength of plaster. Then the reliability of FGM's strength data is examined by applying the concept of the weakest link theory as a first trial. Each fracture strength of plaster in FGMs is possible to evaluate from the macroscopic fracture strength of FGM applying the micro-mechanics⁽⁷⁾.

In the present paper, it is discussed about the method to evaluate the reliability of brittle FGM's strength using plaster-corundum model FGMs. So that, effective volume, which is one of the parameter to compare the strength data of different methods and sizes, is calculated for the tests of 3-point bending, 4-point bending, and ring diametrical compression. It is assumed here that the usual theoretical assumptions for uniform material are able to apply for FGMs. The strength of FGM is statistically discussed based on the effective volume calculated by the stress acted on the plaster that is dominated the fracture of the model FGMs.

2. ANALYSIS AND EXPERIMENTAL METHOD

2.1 Weibull Distribution Function

The FGM is assumed to break according to the weakest link theory proposed by Weibull where the strength of a material is controlled by the growth of the defects in the body of volume V . In case of two-parameter Weibull distribution, the probability function $F(\sigma)$ is;

$$F(\sigma) = 1 - \exp \left\{ \int_V (\sigma/\sigma_o)^m dV \right\} \dots\dots\dots(1)$$

where, m is shape or Weibull parameter and σ_o is scale parameter. If tensile stress field in a specimen is given as a function of maximum tensile stress, σ_t , an effective volume, V_E , is;

$$V_E = \int_V (\sigma/\sigma_t)^m dV \dots\dots\dots(2)$$

Substituting Eq. (2) into Eq. (1);

$$F(\sigma) = 1 - \exp \left\{ -(\sigma_t/\sigma_o)^m V_E \right\} \dots\dots\dots(3)$$

and mean fracture strength, $\bar{\sigma}$, is given as follows;

$$\bar{\sigma} = \sigma_o V_E^{-1/m} \Gamma \left\{ (m+1)/m \right\} \dots\dots\dots(4)$$

where $\Gamma(\cdot)$ is a Gamma function. Thus, relation between effective volume and fracture strength is;

$$\bar{\sigma}_2/\bar{\sigma}_1 = (V_{E1}/V_{E2})^{1/m} \dots\dots\dots(5)$$

where $\bar{\sigma}_1$ and $\bar{\sigma}_2$ are the mean fracture strength having an effective volume of V_{E1} and V_{E2} , respectively.

2.2 Experimental Material and Specimen

The materials tested in the present study are model FGMs made by the centrifugal method utilizing the difference of centrifugal force caused by the difference of density between each component. The combination of materials is plaster as a matrix and corundum powder as dis-

tributed particles having grain size of #60⁽¹⁾. Elastic modulus of bulk plaster and corundum are $E_p \approx 35$ GPa and $E_c \approx 360$ GPa, respectively, and Poisson's ratio are assumed same and constant of $\nu = 1/3$. The tests of 3-point bending, 4-point bending, and ring diametrical compression are done by a screw-driven tension-compression machine with the cross-head speed of 0.1 mm/min. Figure 1 shows the dimension of specimens and those are width $b = 16$ mm, height $h = 14$ mm, and span $L_1 = 25$ mm for 3-point bending specimen, $b = 16$ mm, $h = 14$ mm, upper span $L_1 = 12$ mm and lower span $L_2 = 26$ mm for 4-point bending specimen and outer diameter $D = 90$ mm, inner diameter $d = 60$ mm, thickness $t = 15$ mm, and width $b = 30$ mm for ring diametrical compression specimen. Specimens are dried in room temperature more than three months after formed and are kept in the dryer of 40°C for one day before testing.

Four kinds of the mean volume fraction of corundum R for each specimen are made and are $R = 15$ vol%, 25vol%, 35vol% and 0vol% as standard. The gradation profiles in the radial direction of mold are mathematically arranged as a function of specific thickness, X , where $X = 0$ and $X = 1$ are corresponding to the inner and outer surfaces of the ring, respectively⁽¹⁾ Those functions, $f(X)$, are;

$$f(X) = -13.96X^3 + 20.94X^2 + 11.51 \dots\dots\dots(6)$$

$$f(X) = -80.31X^3 + 120.46X^2 + 4.93 \dots\dots\dots(7)$$

$$f(X) = -131.91X^3 + 197.87X^2 + 2.02 \dots\dots\dots(8)$$

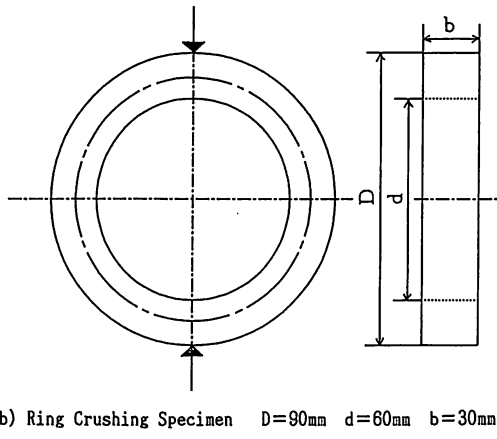
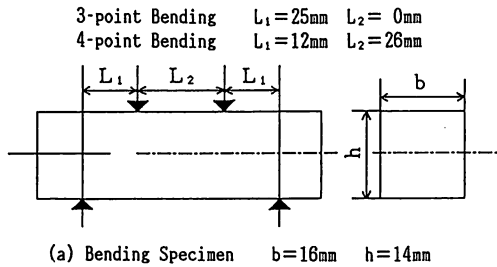


Fig. 1 Configuration of the specimens and the arrows indicate the loading direction.

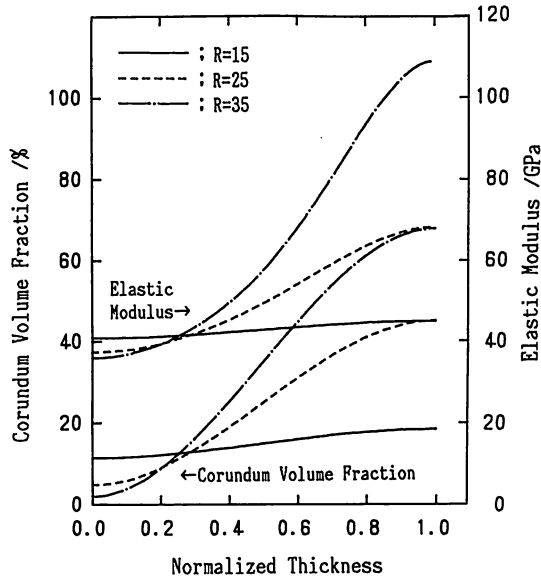


Fig. 2 Gradient distribution of corundum in plaster matrix and corresponding elastic modulus gradation.

for R = 15 vol%, 25 vol% and 35 vol%, respectively. The distribution profiles of corundum powders are shown in Fig. 2. There is a tendency that the gradation increases with an increase of R-value because of a higher applied centrifugal force. Here, cracks for each specimen are always initiated from X = 0 of the inner surface and propagated toward the radial direction of the mold.

The gradient distribution of elastic modulus, E(X), generated by the composition gradation, f(X), is represented by the following equation⁽⁸⁾;

$$E(X) = (1-f) E_p + f E_c - f(1-f)(E_c - E_p)^2 / \{ (f+1/2) E_p + (1-f) E_c \} \dots\dots\dots(9)$$

where $f = f(X)/100$. Variations of elastic modulus are also shown in Fig. 2 and the profiles show the comparable tendency with the composition gradation.

2.3 Stress Field for Bending Test

The bending theory of a straight beam is applied for the evaluation of the stress field of 3-point and 4-point bending specimens. Stress, σ , and strain, ϵ , of some distance, e, from a neutral axis is;

$$\epsilon = e/\gamma \dots\dots\dots(10)$$

$$\sigma = E(X) \cdot \epsilon = E(X) \cdot e/\gamma \dots\dots\dots(11)$$

where γ is the curvature of neutral axis. The condition that a summation of stresses acting over the cross-section, A, is zero gives a relation;

$$\int \sigma dA = \int \{ E(X) \cdot e/\gamma \} dA = 0 \dots\dots\dots(12)$$

And the relation that summation of moment around zz-axis (i.e., width direction) equals to

the applied bending moment M gives the relation;

$$\int (e \cdot \sigma) dA = \int \{E(X) \cdot e^2 / \gamma\} dA = M \quad \dots\dots\dots(13)$$

After all, Eqs. (12) and (13) are written as;

$$\int \{E(X) \cdot e\} dA = 0 \quad \dots\dots\dots(14)$$

$$\gamma = [\int \{E(X) \cdot e^2\} dA] / M \quad \dots\dots\dots(15)$$

respectively. If the bending moment is known, the distribution fields of strain and stress are obtained based on Eqs. (10) and (11), respectively.

2.4 Stress Field for Ring Diametrical Compression Test

The curved beam theory is applied to analyze the stress field of a ring diametrical compression specimen⁽³⁾. The strain, ϵ , and stress, σ , at a point of distance e from a neutral axis of curvature γ is given by;

$$\epsilon = (\gamma \cdot \epsilon_0 + e \cdot \omega_0) / (\gamma + e) \quad \dots\dots\dots(16)$$

$$\sigma = E(X) \cdot \epsilon \quad \dots\dots\dots(17)$$

where ϵ_0 and ω_0 is the longitudinal strain and angular strain, respectively. The tensile load, T , and the bending moment, M , which are components of an applied ring compression load, are balanced with the stresses by Eq. (17) and then the relations are written as;

$$T = \int \sigma dA = \epsilon_0 \int \{E(X) \cdot \gamma / (\gamma + e)\} dA + \omega_0 \int \{E(X) \cdot e / (\gamma + e)\} dA \quad \dots\dots\dots(18)$$

$$M = \int (e \cdot \sigma) dA = \epsilon_0 \int \{E(X) \cdot \gamma \cdot e / (\gamma + e)\} dA + \omega_0 \int \{E(X) \cdot e^2 / (\gamma + e)\} dA \dots\dots(19)$$

Values of ϵ_0 and ω_0 at any radial plane are calculated from a simultaneous equation of Eqs. (18) and (19). Thus, the strain and stress fields are obtained from Eqs. (16) and (17), respectively.

2.5 Calculation of Effective Volume

Numerical calculation is done for the evaluation of the effective volume defined by Eq. (2). Equation (2) is arranged for the easiness of calculation as;

$$V_E \approx \sum \{(\sigma / \sigma_t)^m \Delta V\} \quad \dots\dots\dots(20)$$

In case of 3-point and 4-point bending tests, the finite volume of ΔV is

$$\Delta V = b \cdot \Delta L \cdot \Delta h \quad \dots\dots\dots(21)$$

where ΔL and Δh is the finite increment toward span and height direction of rectangular specimen, respectively. The calculation of the effective volume by Eq. (20) is easily done. Because the border of tensile and compressive stress region is the neutral axis, strains are a simple function of the bending moment, M , which is reduced to Eqs. (10) and (15), and stresses parallel to a load axis are in proportion to the bending moment at the position.

While a simple relation is not held in ring specimens. The volume is divided into the finite volume of ΔV at an angle increment, $\Delta \theta$, from a loading axis and a radius increment, Δr , from an inner plane of the ring;

$$\Delta V = b \cdot \gamma \Delta \theta \cdot \Delta \gamma \quad \dots\dots\dots(22)$$

The stress distribution in the ring specimen are different qualitatively depending on a position of a radial plane because the tensile load, T, and the bending moment, M, vary as a function of angle, θ , from the loading axis. Therefore, it is necessary to calculate an average stress acted on each finite volume of ΔV different from the bending test. Thus the effective volume can be estimated by applying Eq. (20).

2.6 Separation of Stress Applied on FGM

The stress applied on FGM can be divided into stress components for plaster and corundum based on the micro-mechanics⁽⁷⁾. When solid circular particles are distributed in matrix, the vector representation of stress components for a matrix $\{\sigma_m\}$ and a particle $\{\sigma_p\}$ are given as ;

$$\{\sigma_m\} = \mathbf{B}_p [\mathbf{B}_p^{\circ-1} \{\bar{\sigma}\}] \quad \dots\dots\dots(23)$$

$$\{\sigma_p\} = \mathbf{B}_p \{\bar{\sigma}\} \quad \dots\dots\dots(24)$$

respectively. Where $\{\bar{\sigma}\}$ is macroscopic applied stress components and ;

$$\mathbf{B}_p = [\mathbf{I} - (1-f) \mathbf{L}_m (\mathbf{S}_p - \mathbf{I}) (\mathbf{C}_p - \mathbf{C}_m)]^{-1} \quad \dots\dots\dots(25)$$

$$\mathbf{B}_p^{\circ} = [\mathbf{I} - \mathbf{L}_m (\mathbf{S}_p - \mathbf{I}) (\mathbf{C}_p - \mathbf{C}_m)]^{-1} \quad \dots\dots\dots(26)$$

and \mathbf{I} is the 4th unit tensor ;

$$\mathbf{I}_{ijkl} = \delta_{ik} \delta_{jl} + \delta_{il} \delta_{jk} \quad \dots\dots\dots(27)$$

where δ is Cronecker delta and \mathbf{L} stiffness tensor (i.e., $\{\sigma\} = \mathbf{L}\{\epsilon\}$), \mathbf{S} Eshelby tensor⁽⁹⁾ and \mathbf{C} elastic compliance (i.e., $\{\epsilon\} = \mathbf{C}\{\sigma\}$). Those values used in the present analysis are given in Appendix. So the effective volume is calculated to insert the stresses given by Eq. (23) into corresponding σ and σ_t terms of Eq. (20) as mentioned in Sec. 2.5.

3. RESULTS AND DISCUSSION

3.1 Stress Distribution and Gradient Composition

The specific stress distributions normalized with respect to maximum tensile stress are shown in Figs. 3 and 4 for the evaluation of the effect of a gradient distribution on the stress field. Fig. 3 shows profiles of stress distribution along a loading axis of 3-point and 4-point bending tests. Both normalized results are coincided with each other because the difference of a bending moment is vanished by normalization. The stress distribution profile of the ring specimen is depended on the angular position of a radial plane. Figure 4 shows the stress distribution profiles along the loading axis for ring diametrical compression test where yield the maximum tensile stress and also yield the maximum stress gradation⁽³⁾. The average of a specific tensile stress is increased with an increase of R-value and a deviation of the stress distribution from R = 0 curve for Fig. 4 is less than that for Fig. 3. In a ring diametrical compression test, tensile stresses are generated in four regions which are upper and lower inside regions on a loading axis and left and right outside regions normal to the loading axis. However, failure always initiate from the inner radial plane along the loading axis so that both

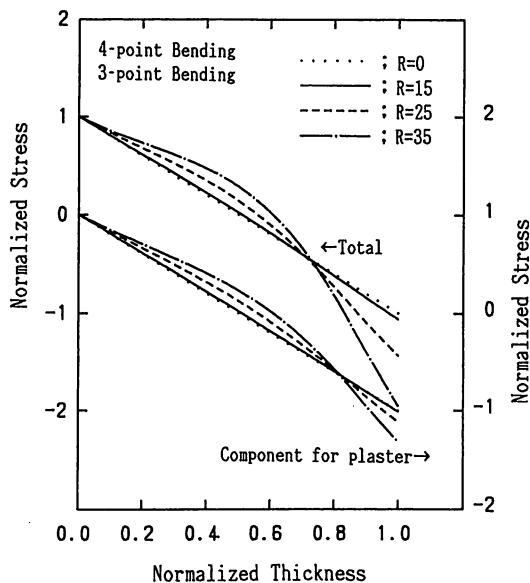


Fig. 3 Distribution of total applied stress and stress acted on plaster for 3-point and 4-point bending tests.

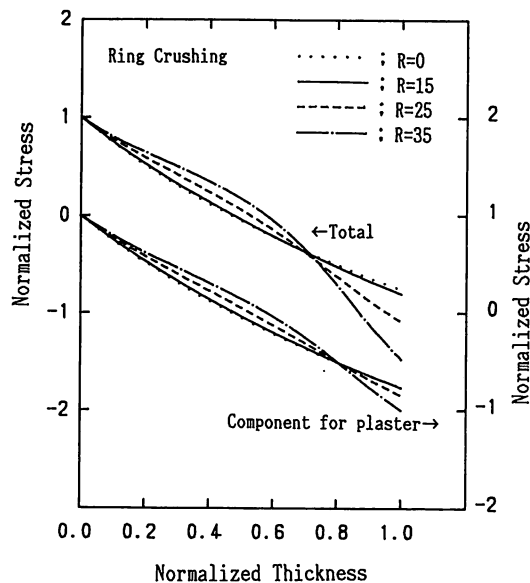


Fig. 4 Distribution of total applied stress and stress acted on plaster for ring diametrical compression tests.

outside regions are omitted for the calculation in the present study.

3.2 Effective Stress for Fracture

The fracture strength of plaster is quite weak compared with that of corundum and then plaster dominates the fracture of plaster-corundum model FGM⁽³⁾. In this situation, it seems to be proper to evaluate the effective volume with respect to the stress only worked on plas-

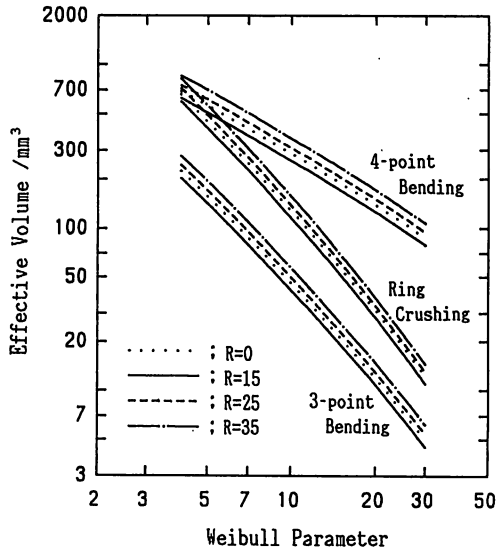


Fig. 5 Effect of Weibull parameter on effective volume of specimens.

ter which is divided the total applied stress according to the method mentioned in Sec. 2.6. The distribution of specific stress worked on plaster is also shown in Figs. 3 and 4, where stresses are normalized with the maximum tensile stress. The deviation of a stress distribution for each curve from $R=0$ curve is smaller compared with total ones mentioned in Sec. 3.1. The dependence of effective volumes on Weibull parameter, m , is checked in a range $m = 4 \sim 30$ and the results are shown in Fig. 5. The dependence of effective volumes on the composition gradation is recognized as follows; the effective volume as a function of the composition gradation is decreased in the first time and then increased compared with a homogeneous one. Moreover, the effective volumes become large in the order of 3-point bending, ring diametrical compression, and 4-point bending tests and these values are seemed to be proper for the discussion of the size effect.

3.3 Fracture Stress and Effective Volume

Fracture stresses are calculated from a fracture load followed by the method mentioned in Sec. 2.3 and Sec. 2.4. The fracture strength are plotted on the Weibull probability paper as shown in Fig. 6. The data number of each group is 50 to 60 points and the variation between each data line for bending tests seems to be greater compared with that for ring compression tests. Each data set makes each straight line having no obvious transition point. So that they seem to be obeyed two-parameter Weibull distribution and the lines for the calculation of parameters are obtained by a least square method. These parameters of Weibull parameter (i.e., shape parameter), scale parameter, mean strength, variance and coefficient of variation are summarized in Table 1. Any dependence of Weibull parameter on the composition gradation is not obvious. The average of Weibull parameter is $m = 7.7$ (≈ 8) and the small m -value means that the strength data have a relatively large deviation.

Figure 7 shows the relation between an effective volume for $m = 8$ and plaster fracture stress which is calculated based on equations shown in Sec. 2.6. Each data set plot the maxi-

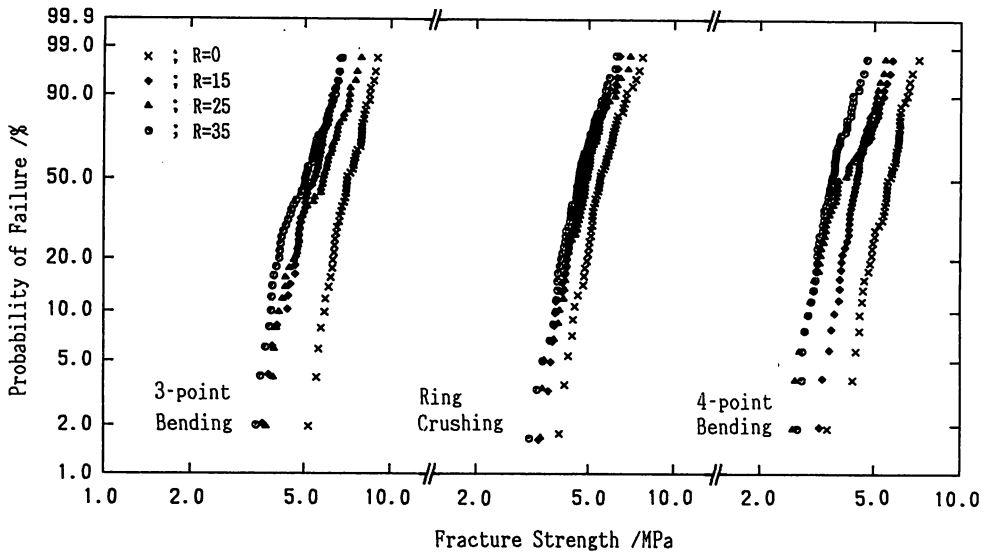


Fig. 6 Comparisons of Weibull plots of fracture strength for tests of 3-point bending, 4-point bending, and ring diametrical compression.

Table 1 Summary of Weibull parameter.

Test Method	m	σ_0	$\bar{\sigma}$	v	η
R = 0 (Plaster) Specimen					
3-point Bending	8.65	7.57	7.15	0.97	0.138
Ring Crushing	7.63	5.97	5.61	0.76	0.155
4-point Bending	8.20	5.88	5.55	0.65	0.145
R = 15 Specimen					
3-point Bending	7.76	5.64	5.30	0.65	0.153
Ring Crushing	7.77	5.14	4.84	0.54	0.152
4-point Bending	8.30	4.68	4.42	0.40	0.143
R = 25 Specimen					
3-point Bending	6.17	6.15	5.68	1.35	0.204
Ring Crushing	7.29	5.27	4.94	0.64	0.162
4-point Bending	6.18	4.30	3.98	0.66	0.204
R = 35 Specimen					
3-point Bending	6.58	5.39	5.00	0.92	0.191
Ring Crushing	7.67	4.95	4.65	0.51	0.154
4-point Bending	8.72	3.79	3.59	0.24	0.137

m; Shape Parameter, σ_0 ; Scale Parameter (MPa)
 $\bar{\sigma}$; Mean Strength (MPa), v; Variance
 η ; Coefficient of Variation

imum, minimum and average values and plot points are within two dotted lines. The fracture stress is decreased with an increase of effective volume that is the order of 3-point bending,

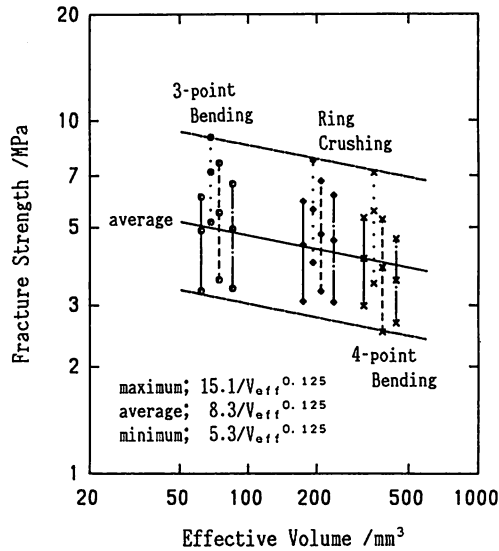


Fig. 7 Relation between fracture strength and effective volume for Weibull parameter $m=8.0$.

ring diametrical compression and 4-point bending tests. The solid line in Fig. 7 shows the mean value of fracture stress and obeys Eq. (5) as;

$$\bar{\sigma} = 8.3V_E^{-0.125} \dots\dots\dots(28)$$

Again, here assumed the strength of a plaster-corundum model FGM is controlled by the fracture of weaker plaster and then the effective volumes concerning with the stress acted on only plaster are calculated. The assumption seems to be proper judging from a relation of Eq. (28) and plaster-corundum model FGM has the size effect. While the strength of plaster-corundum model FGM for any volume and composition gradation can be evaluated using Eq. (28).

4. CONCLUSIONS

Plaster-corundum FGM specimens having four kinds of composition gradation are made and three kinds of tests, which were 3-point bending, 4-point bending and ring diametrical compression tests, are done for the purpose to offer one of the concept how to consider and treat the reliability of strength data in FGMs. The data of strength are summarized based on the effective volume of the specimen and the following results are obtained.

- (1) The fracture strength of each composition gradation and each test method can adopted the two parameter Weibull distribution.
- (2) The greater composition gradation gives the bigger effective volume of specimen.
- (3) Weibull parameter seems to be independent of the composition gradation and the small average value of $m=8$ is obtained.
- (4) Size effect that the bigger effective volume gives the smaller fracture strength is observed and the mean strength of plaster is arranged as $\bar{\sigma}=8.3V_E^{-0.125}$.

5. REFERENCES

- (1) Y. Fukui, JSME Int. J., Ser. III, Vol. 34, No. 1 (1991), 144.
- (2) Y. Fukui, Y. Oya-Seimiya, and K. Nakanishi, JSME. J., Ser. A, Vol. 57, No. 540 (1991), 1790.
- (3) Y. Fukui, H. Kinoshita and K. Nakanishi, JSME Int. J., Ser. I, Vol. 35, No. 1 (1992), 95.
- (4) M. Ichikawa *et.al.*, "Fracture Strength", (1985), 93, ohmu-sha, Tokyo.
- (5) K. Matsuo *et.al.*, "Evaluation of mechanical properties of Ceramics", (1986), 41, Nikkan Kogyo Shinbun-sha, Tokyo.
- (6) Y. Taniguchi and J. Kitazumi, J, Mater. Sci., Japan, Vol. 38, No. 435 (1989), 1428.
- (7) K. Wakashima and H. Tsukamoto, Proc. 1st Int. Sympo. FGM, (1990), 19.
- (8) K. Wakashima, Trans. Jpn. Soc. Comp. Mater, Vol. 2, No. 4 (1976), 161.
- (9) J. D. Eshelby, Proc. Roy. Soc. (London), Vol. 241 A (1957), 376.

APPENDIX

In case of Poisson's ratio $\nu = 1/3$, the Eshelby tensor⁽⁹⁾ **S**, the stiffness tensor **L** and the elastic compliance **C** shown in Sec. 2.6 are given as follows;

$$\mathbf{S} = \begin{vmatrix} S_1 S_2 S_2 & 0 & 0 & 0 \\ S_2 S_1 S_2 & 0 & 0 & 0 \\ S_2 S_2 S_1 & 0 & 0 & 0 \\ 0 & 0 & 0 & S_3 & 0 & 0 \\ 0 & 0 & 0 & 0 & S_3 & 0 \\ 0 & 0 & 0 & 0 & 0 & S_3 \end{vmatrix} \dots\dots\dots(\text{A-1})$$

where $S_1 = (7-5\nu)/15(1-\nu) = 8/15$, $S_2 = -(1-5\nu)/15(1-\nu) = 1/15$, and $S_3 = (4-5\nu)/15(1-\nu) = 7/30$.

$$\mathbf{L} = \begin{vmatrix} L_1 L_2 L_2 & 0 & 0 & 0 \\ L_2 L_1 L_2 & 0 & 0 & 0 \\ L_2 L_2 L_1 & 0 & 0 & 0 \\ 0 & 0 & 0 & L_3 & 0 & 0 \\ 0 & 0 & 0 & 0 & L_3 & 0 \\ 0 & 0 & 0 & 0 & 0 & L_3 \end{vmatrix} \dots\dots\dots(\text{A-2})$$

where $L_1 = (1-\nu^2)E/(1-3\nu^2-2\nu^3) = 3E/2$, $L_2 = (\nu + \nu^2)E/(1-3\nu^2-2\nu^3) = 3E/4$ and $L_3 = G = E/2(1+\nu) = 3E/8$.

$$\mathbf{C} = \begin{vmatrix} C_1 C_2 C_2 & 0 & 0 & 0 \\ C_2 C_1 C_2 & 0 & 0 & 0 \\ C_2 C_2 C_1 & 0 & 0 & 0 \\ 0 & 0 & 0 & C_3 & 0 & 0 \\ 0 & 0 & 0 & 0 & C_3 & 0 \\ 0 & 0 & 0 & 0 & 0 & C_3 \end{vmatrix} \dots\dots\dots(\text{A-3})$$

where $C_1 = 1/E$, $C_2 = -\nu/E = -1/3E$ and $C_3 = 1/G = 2(1+\nu)/E = 8/3E$.